© The American Society of Gene & Cell Therapy

Sonic Hedgehog Expands Diaphyseal Trabecular Bone Altering Bone Marrow Niche and Lymphocyte Compartment

Maija Kiuru[1], Chisa Hidaka[1,2], Ralf-Harto Hubner[1], Jason Solomon[2], Anja Krause[1], Philip L Leopold[1] and Ronald G Crystal[1]

[1]Department of Genetic Medicine, Weill Medical College of Cornell University, New York, New York, USA; [2]Laboratory for Soft Tissue Research, The Hospital for Special Surgery, New York, New York, USA

Bone marrow contains distinct microenvironments that regulate hematopoietic stem cells (HSCs). The endosteal HSC niche includes osteoblasts, mineral, and extracellular matrix proteins that interact through various molecular signals to control HSCs. Sonic hedgehog (Shh) is a morphogen involved in the regulation of skeletal development and hematopoiesis, but the effects of Shh on bone in relation to the HSC niche are not well understood. We demonstrate that systemic overexpression of Shh in mice increases osteoblast number with the resultant formation of new trabeculae in the femoral diaphysis. Suggestive of a functional change in the hematopoietic niche, numbers of Lin^- $Sca\text{-}1^+$ $c\text{-}Kit^+$ cells with hematopoietic progenitor function expand, although cells with *in vivo* repopulating capacity in the wild-type environment do not increase. Instead, Shh mediates a decrease in number of bone marrow lymphocytes accompanied by a decreased expression of stromal-derived growth factor 1 (SDF-1) and a decrease in Flk2-expressing Lin^- $Sca\text{-}1^+$ $c\text{-}Kit^+$ cells, indicating a modulation of early lymphopoiesis. This is caused by a microenvironment-induced mechanism as Shh treatment of bone marrow recipients, but not donors, results in a dramatic depletion of lymphocytes. Together, these data suggest that Shh mediates alterations in the bone marrow hematopoietic niche affecting the early lymphoid differentiation.

Received 28 July 2008; accepted 3 April 2009; published online 12 May 2009. doi:10.1038/mt.2009.102

INTRODUCTION

Hematopoiesis is maintained by hematopoietic stem cells (HSCs) that are able to self-renew and differentiate into all mature hematopoietic lineages. A critical component in the regulation of HSCs is the stem cell niche, the microenvironment within bone marrow that provides the physical interaction and inhibitory and stimulatory signals required to maintain HSC numbers, and to modulate the HSC response to changes in physiological conditions.[1–3] HSCs reside in the bone marrow in the proximity of the endosteal surfaces of bones in close contact with osteoblasts or close to marrow sinusoidal vessels.[3,4] Current concepts suggest that it is the combination of endosteal bone surface, mineral content, osteoblasts, stromal cells, and extracellular matrix proteins, that controls the maintenance and differentiation of HSCs in the marrow.[1–3]

The signaling networks involved in the regulation of HSCs include the Wnt, Notch, bone morphogenetic protein, and hedgehog pathways, as well as molecules including N-cadherin, parathyroid hormone, hyaluronic acid, osteopontin, angiopoietin-1, and Kit ligand.[1–3,5–7] Of these, we focused on Sonic hedgehog (Shh), a secreted morphogen that mediates cell differentiation in a variety of embryonic and adult tissues. Although Shh is well known to be involved in the development of skeletal and hematopoietic systems,[5,8–17] the effects of Shh on bone in relation to the HSC niche and HSCs, particularly in postnatal animals, are not well understood. As hedgehog signaling has been shown to regulate the expansion of HSCs in adult organisms,[5,17–19] we hypothesized that Shh is a regulator of the bone marrow endosteal niche, and consequently affects the HSC number and function in the postnatal bone marrow.

Our experimental strategy was to transiently elevate systemic levels of Shh in mice by administering AdShhN, an adenovirus (Ad) gene transfer vector coding for the 19 kd N-terminal portion of Shh that is responsible for all of the biological effects of Shh.[20,21] The C-terminal portion of the AdShhN coding sequence was modified to prevent the covalent attachment of cholesterol, enhancing the diffusion of Shh through tissues.[20,22] The results demonstrate that Shh mediates an increase in osteoblasts and the appearance of new trabeculae in the femoral diaphysis of mice. Concomitantly, the number of Lin^- $Sca\text{-}1^+$ $c\text{-}Kit^+$ cells with hematopoietic progenitor function is increased, although cells with *in vivo* repopulating capacity in the wild-type environment do not increase. Instead, Shh mediates decreases in numbers of bone marrow lymphocytes and lymphoid engraftment by a microenvironment-induced effect. Together, the data show that Shh is a regulator of the bone marrow hematopoietic niche, likely impairing the early lymphocyte development resulting in depletion of the bone marrow lymphocyte compartment.

Correspondence: *Ronald G Crystal, Department of Genetic Medicine, Weill Cornell Medical College, 1300 York Avenue, Box 96, New York, New York 10065, USA. E-mail: geneticmedicine@med.cornell.edu*

© The American Society of Gene & Cell Therapy

RESULTS

Systemic delivery of Shh with intravenous administration of AdShhN

Our previous studies showed that administration of AdShhN to mice provides a transient (3 weeks) augmentation of Shh levels.[20,21] As systemic administration of Ad via a peripheral vein results in elevated serum levels of the protein product primarily due to transgene expression in the liver; 5 days after AdShhN was administered intravenously to 6–8-week-old C57BL/6 mice, the serum of AdShhN-treated mice, but not phosphate-buffered saline (PBS) or AdNull (an identical Ad vector without the ShhN cDNA) treated mice, showed high levels of murine Shh (**Supplementary Figure S1a**; $P < 0.05$, AdShhN versus both controls) (see **Supplementary Materials and Methods**). Based on our previous studies showing that Ad-mediated expression of Shh induces anagen, the active phase of hair follicle cycling,[21] mice were assessed for hair growth. Gross examination and histology of AdShhN-treated mice showed induction of anagen as previously described confirming the activity of Shh (**Supplementary Figure S1b,c**).[20,21]

Administration of AdShhN induces the formation of new trabeculae in diaphyseal bone

To examine the effect of systemic elevation of Shh levels on bone *in vivo*, femurs were harvested 18 days after vector administration and analyzed by brightfield microscopy. Hematoxylin and eosin–stained sections of femurs from AdShhN-treated mice displayed a marked increase in trabecular bone in the bone marrow cavity of the femoral diaphysis (**Figure 1a**) with increased endosteal surface (**Figure 1a**, middle panels). Quantitative analysis confirmed that AdShhN-treated mice had a significant increase in trabecular area (**Figure 1b**; $P < 0.0001$, AdShhN versus both controls), trabecular perimeter (**Figure 1c**; $P < 0.0001$, AdShhN versus both controls) (see **Supplementary Materials and Methods**), and endosteal tortuosity ratio (endosteal surface length divided by bone length; **Figure 1d**; $P < 0.001$, AdShhN versus both controls). The trabeculae were also present in femurs harvested 30 days after vector administration but disappeared by 8 months (**Supplementary Figure S2a,b**). In addition, serum osteocalcin level, a marker for new bone formation, was significantly

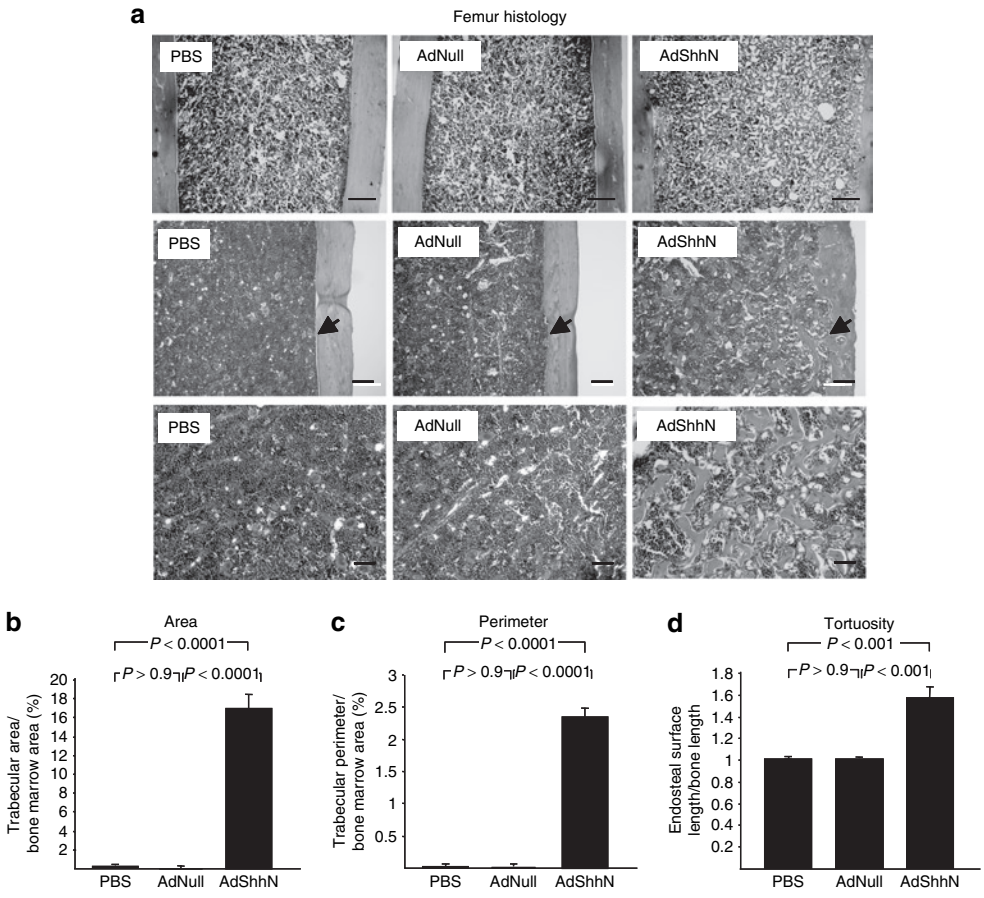

Figure 1 Appearance of new trabeculae in femoral diaphysis induced by elevated levels of Sonic hedgehog (Shh). Femurs were harvested 18 days after intravenous administration of an adenovirus vector encoding a soluble form of Shh (AdShhN), a control vector with no transgene (AdNull), or vehicle (phosphate-buffered saline, PBS) to C57BL/6 mice, fixed and stained with hematoxylin and eosin (H&E) and examined by brightfield microscopy. (**a**) H&E images of femurs: PBS (left panels), AdNull (middle panels), and AdShhN (right panels). For middle panels, arrow points at the endosteal surface. For upper panels, bar = 200 μm; for middle panels, bar = 100 μm; and for lower panels, bar = 50 μm. (**b–d**) Quantification of diaphyseal trabecular bone. Measurements were made on H&E images, $n = 5$ measurements/mouse, $n = 5$ mice/group. (**b**) Percentage of trabecular area/bone marrow area in the femoral diaphysis; (**c**) percentage of trabecular perimeter/bone marrow area in the femoral diaphysis; and (**d**) tortuosity ratio (endosteal surface length/bone length) of femur endosteal surface. For **b–d**, data shown as mean ± SE.

© The American Society of Gene & Cell Therapy

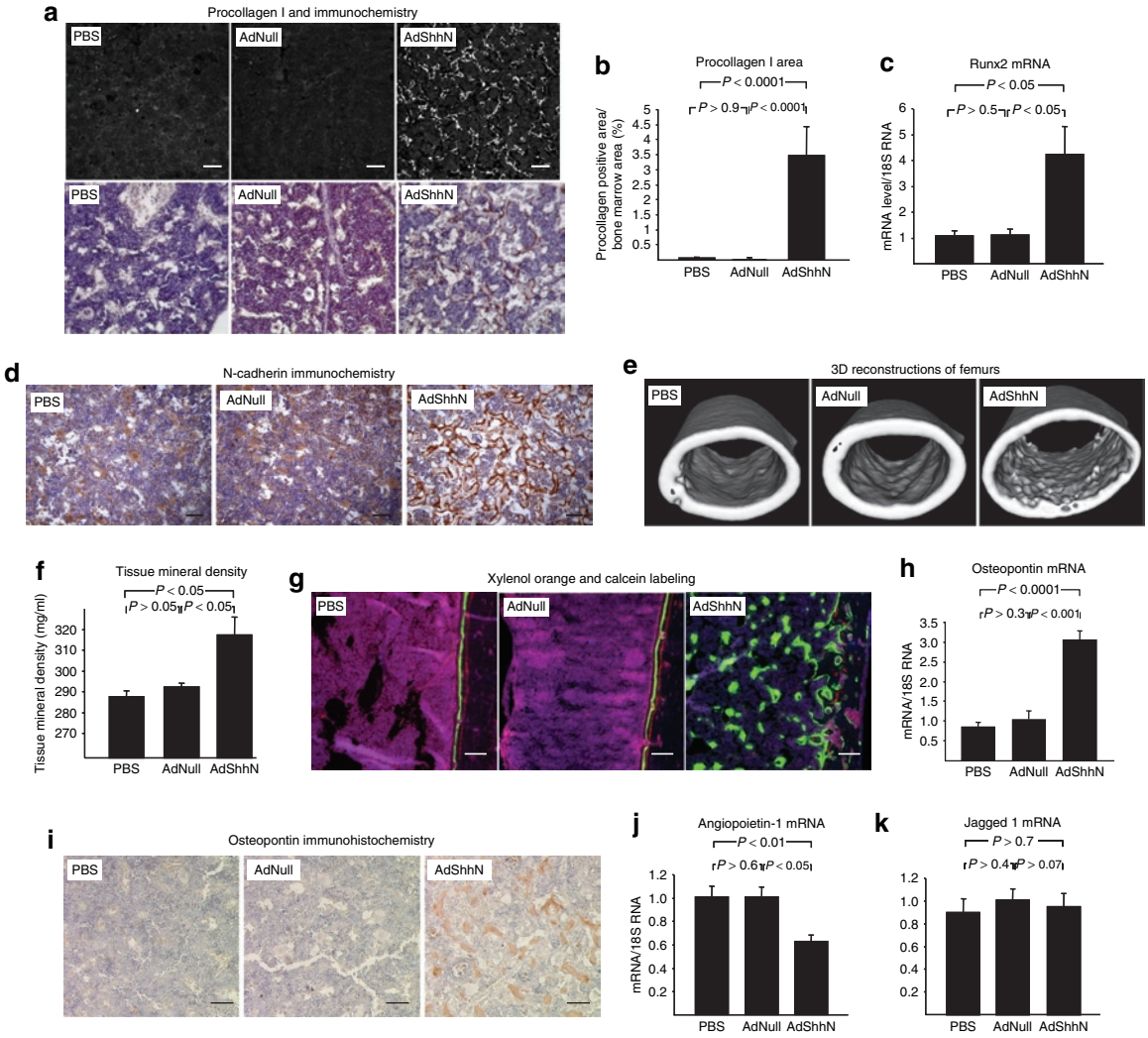

Figure 2 Changes in the bone marrow hematopoietic niche components in the bone marrow of AdShhN-treated mice. Analyses were carried out in femurs and/or tibias 18 days after vector administration. (**a**) Immunofluorescence and immunohistochemistry staining of femurs with antibody against procollagen type I, a marker of osteoblasts: phosphate-buffered saline (PBS) (left); AdNull (middle); and AdShhN (right). For upper panels, white indicates positive staining (a grayscale image of immunofluorescence staining). Bar = 100 μm. For lower panels, brown indicates positive staining. Bar = 50 μm. (**b**) Percentage of procollagen type I positive area/bone marrow area in the femoral diaphysis (five measurements/mouse, five mice/group). (**c**) Runx2 mRNA expression ($n = 4$, each condition). RNA was extracted from tibial bone marrow cells and relative quantification of gene expression was analyzed by TaqMan real-time PCR. (**d**) Immunohistochemical staining of femurs with antibody against N-cadherin: PBS (left); AdNull (middle); and AdShhN (right). Bar = 50 μm. Brown indicates positive staining. (**e**) Examples of 3D images of femoral diaphyses by micro-computed tomography: PBS (left); AdNull (middle); and AdShhN (right). The increased tortuosity of the bone endosteal surface is apparent in the right panel. (**f**) Tissue mineral density in the femoral diaphysis excluding cortical bone (PBS, $n = 3$; AdNull, $n = 4$; AdShhN, $n = 5$) as measured in micro-computed tomography images. Although the resolution >17 μm is not sufficient to visualize trabecular bone within the marrow space, increased tissue mineral density in the femoral diaphysis was detected in AdShhN-treated animals. (**g**) Active mineralization of trabeculae in the diaphysis of AdShhN-treated animals. Mice were injected with xylenol orange and calcein, which are deposited at active sites of mineralization, 4 days and 1 day before killing, respectively. PBS (left), AdNull (middle), and AdShhN (right). Xylenol orange (red), calcein (green), and autofluorescence (purple). Bar = 100 μm. (**h–k**) Gene expression changes in the bone marrow of AdShhN-treated animals. (**h**) Osteopontin mRNA levels ($n = 4$, each condition); (**i**) osteopontin protein expression; (**j**) angiopoietin-1 mRNA levels (PBS, $n = 4$; AdNull, $n = 5$; AdShhN, $n = 5$); and (**k**) Jagged 1 mRNA levels ($n = 4$, each condition). For **b,c,f** and **h,j,k**, data shown as mean ± SE. Ad, adenovirus; Runx2, runt-related transcription factor 2; Shh, Sonic hedgehog.

increased in Shh-treated mice 18 days after vector administration (**Supplementary Figure S3**; $P < 0.0001$, AdShhN versus both controls) (see **Supplementary Materials and Methods**). These data demonstrate that systemic elevation of Shh levels results in the formation of new trabeculae in the diaphyseal trabecular bone and an increase in the endosteal surface area, increasing the site of the HSC niche.

Alterations in the structure of the bone marrow niche after administration of AdShhN

To further characterize the Shh-induced changes in the structure of the endosteal HSC niche, we analyzed known components of the niche. First, as osteoblasts are an essential component of the HSC microenvironment,[23,24] we quantified osteoblasts by procollagen type I staining and found a marked

© The American Society of Gene & Cell Therapy

increase in osteoblasts in the femoral diaphysis (see **Figure 2a** for example; **Figure 2b** for quantification; $P < 0.0001$, AdShhN versus both controls) (see **Supplementary Materials and Methods**). Although type I collagen is an extracellular matrix protein, the antibody recognizes the procollagen form of the protein, before secretion to the extracellular matrix, localizing to the osteoblasts. The osteoblasts displayed spindle-shaped fibroblast-like morphology instead of cuboidal form typical for mature osteoblasts,[25] suggesting an increase in immature osteoblasts. Supporting the data, mRNA expression of runt-related transcription factor 2 (Runx2, also known as core-binding factor α 1, or Cbfα1), a transcription factor that is a marker for early osteoblastic cells,[26] was elevated (**Figure 2c**; $P < 0.05$, AdShhN versus both controls) (see **Supplementary Materials and Methods**). The osteoblasts also expressed N-cadherin (**Figure 2d**). The spindle-shaped N-cadherin$^+$ osteoblasts are associated with the HSC niche,[24] although it remains controversial whether HSCs depend on N-cadherin-mediated interactions to osteoblasts.[27] Second, as calcium gradients around areas of bone remodeling affect engraftment and retention of HSCs to the endosteal niche,[1,28] we analyzed bone mineralization. Micro-computed tomography (see **Figure 2e** for example) showed an increase in the inner perimeter of the femoral diaphysis in AdShhN-treated mice (PBS, 3.86 ± 0.09 mm; AdNull, 3.90 ± 0.03 mm; AdShhN, 4.26 ± 0.10 mm; $P < 0.05$, AdShhN versus both controls) as well as an increase in tissue mineral density in the femoral diaphysis excluding the cortical bone (**Figure 2f**; $P < 0.05$, AdShhN versus both controls). Active mineralization was also detected by labeling the mineralization front of the bone by intraperitoneal injections of xylenol orange and calcein 4 days and 1 day before killing, respectively (see **Figure 2g** for example). Surprisingly, decreased tissue mineral density was detected in the distal metaphysis of the femurs (distal metaphysis: PBS, 508 ± 8 mg/ml; AdNull, 525 ± 19 mg/ml; AdShhN, 456 ± 11 mg/ml; $P < 0.05$, AdShhN versus PBS; $P < 0.01$, AdShhN versus AdNull; proximal metaphysis: PBS, 547 ± 5 mg/ml; AdNull, 565 ± 7 mg/ml; AdShhN, 527 ± 11 mg/ml; $P > 0.1$, AdShhN versus PBS; $P < 0.05$, AdShhN versus AdNull). In these areas with pre-existing trabeculae, AdShhN appeared to increase surface area at the expense of bone density, with more numerous, but smaller trabeculae apparent in histologic sections. Third, the expression of osteopontin was assessed, as it is an important extracellular matrix component of the niche, functioning to constrain HSC proliferation.[29,30] Expression of osteopontin mRNA and protein was markedly increased in the bone marrow of AdShhN-treated mice (**Figure 2h**; $P < 0.0001$, AdShhN versus PBS; $P < 0.001$, AdShhN versus AdNull; see **Figure 2i** for example of protein expression). Finally, mRNA expression of the HSC niche–associated molecules angiopoietin-1 and Jagged 1 in the bone marrow cells was assessed with the knowledge that angiopoietin-1 is reported to regulate HSC quiescence[31] and Jagged 1 to regulate HSC function through interaction with its ligand Notch.[23] Interestingly, angiopoietin-1 mRNA expression was decreased in AdShhN-treated mice (**Figure 2j**; $P < 0.01$, AdShhN versus PBS; $P < 0.05$, AdShhN versus AdNull), but no change in the marrow Jagged 1 mRNA levels was detected (**Figure 2k**; $P > 0.7$, AdShhN versus both controls). Together, these data suggest an alteration in the structure of the bone marrow microenvironment including remodeling of the existing trabeculae in metaphyseal bone and the appearance of new trabeculae in diaphyseal bone with an increase in osteoblasts, mineralization, and N-cadherin and osteopontin expression.

Increase in primitive hematopoietic compartment and decrease in the number of lymphocytes in the bone marrow of AdShhN-treated mice

To test whether the Shh-mediated structural changes in the bone marrow alter the niche function, the number of bone marrow primitive hematopoietic cells with Lin$^-$ Sca-1$^+$ c-Kit$^+$ immunophenotype was quantified. Assessment of femoral bone marrow cells harvested 18 days after vector administration demonstrated that AdShhN-treated mice had an increase in the percentage of Lin$^-$ Sca-1$^+$ c-Kit$^+$ cells/total bone marrow nucleated cells (**Figure 3a**; $P < 0.01$, AdShhN versus PBS; $P < 0.0001$, AdShhN versus AdNull). Due to a trend of a decrease in the total number of marrow cells recovered from AdShhN-treated mice (**Supplementary Figure S4a**; $P > 0.3$, AdShhN compared to both controls), the total number of Lin$^-$ Sca-1$^+$ c-Kit$^+$ cells was not statistically significant (**Supplementary Figure S4b**; $P > 0.1$, AdShhN versus both controls).

As Lin$^-$ Sca-1$^+$ c-Kit$^+$ cells consist of distinct subpopulations of HSCs, including HSCs capable of bone marrow reconstitution as well as multipotential hematopoietic progenitor cells,[3] we tested whether the increase is due to HSCs or hematopoietic progenitors. To assess the hematopoietic progenitor function, colony-forming unit assay was performed. Cells from AdShhN-treated mice had an increase in marrow progenitor colonies (**Figure 3b**; $P < 0.0001$, AdShhN versus PBS; $P < 0.01$, AdShhN versus AdNull) (see **Supplementary Materials and Methods**). To assess HSCs, we first conducted a long-term culture-initiating cell (LTC-IC) assay by culturing Lin$^-$ cells from AdShhN-treated mice on naive marrow stromal cells, but found no differences in the frequency of colony formation compared to controls (**Figure 3c**; $P > 0.3$, AdShhN versus both controls) (see **Supplementary Materials and Methods**). To validate the data *in vivo*, we performed a competitive transplantation assay by transplanting cells from C57BL/6 (CD45.2) donor mice treated 18 days before with PBS, AdNull, or AdShhN to lethally irradiated naive B6.SJL (CD45.1) recipients (see **Figure 3d** for experimental design). The donor cells were mixed in a 1:1 ratio with congenic cells of the recipient strain. The results showed no significant differences in donor cell engraftment in myeloid or lymphoid lineages in peripheral blood 5 or 8 weeks after transplantation or in bone marrow 10 weeks after transplantation (**Figure 3e**; AdShhN $P > 0.05$ compared with both controls). As downstream activation of the hedgehog pathway is shown to result in decreased cycling of HSCs leading to HSC exhaustion over time,[17] we performed a cell cycle analysis in Lin$^-$ cells 18 days after AdShhN administration. Consistent with the previous report, a decrease in the percentage of Lin$^-$ cells in G2/M phase was detected in AdShhN-treated animals (**Supplementary Figure S5a**; $P < 0.05$, AdShhN versus PBS; $P < 0.01$, AdShhN versus AdNull).

To further assess the Shh-mediated changes in the HSC population, we assessed Flk2 (fms-related tyrosine kinase 3, Flt3)

© The American Society of Gene & Cell Therapy

expression in Lin$^-$ Sca-1$^+$ c-Kit$^+$ cells, as Flk2 is expressed on short-term HSCs, multipotent progenitors, as well as common lymphoid progenitors but not long-term HSCs.[32–34] Surprisingly, the results demonstrated a decrease in the percentage of Flk2 expression in Lin$^-$ Sca-1$^+$ c-Kit$^+$ cells in AdShhN-treated mice (**Figure 3f**; $P < 0.05$, AdShhN versus PBS; $P < 0.01$, AdShhN versus AdNull) and the percentage of Flk2$^-$ Lin$^-$ Sca-1$^+$ c-Kit$^+$ cells was significantly increased (**Figure 3g**; $P < 0.0001$, AdShhN versus PBS; $P < 0.0001$, AdShhN versus AdNull). As no changes were detected in HSC numbers in the LTC-IC assay, competitive repopulation assay, or the percentage of Lin$^-$ CD34$^-$ Sca-1$^+$ c-Kit$^+$ cells (**Supplementary Figure S5b**; AdShhN $P > 0.05$ versus both controls), the decrease in Flk2 expression may suggest a decrease in common lymphoid progenitors.

To further investigate Shh overexpression–mediated changes in lineage differentiation, we analyzed hematopoietic lineages in the bone marrow of mice 18 days after AdShhN administration. Results from staining with lineage antibodies against granulocytes, monocytes, B lymphocytes, and T lymphocytes followed by flow cytometry showed a 40% decrease in the percentage of B lymphocytes (**Figure 3h**; $P < 0.001$, AdShhN versus both controls) and a 35% decrease in T lymphocytes (**Figure 3h**; $P < 0.01$, AdShhN versus both controls). As one of the mechanisms supporting B lymphocyte proliferation is mediated by lymphoid enhancer–binding factor 1 (Lef1), a member of Lef/Tcf transcription factor family of the Wnt pathway, we analyzed Lef1 expression in the bone marrow of Shh-treated mice.[35] Consistent with the reduction in B-lymphocyte numbers, Lef1 expression was significantly

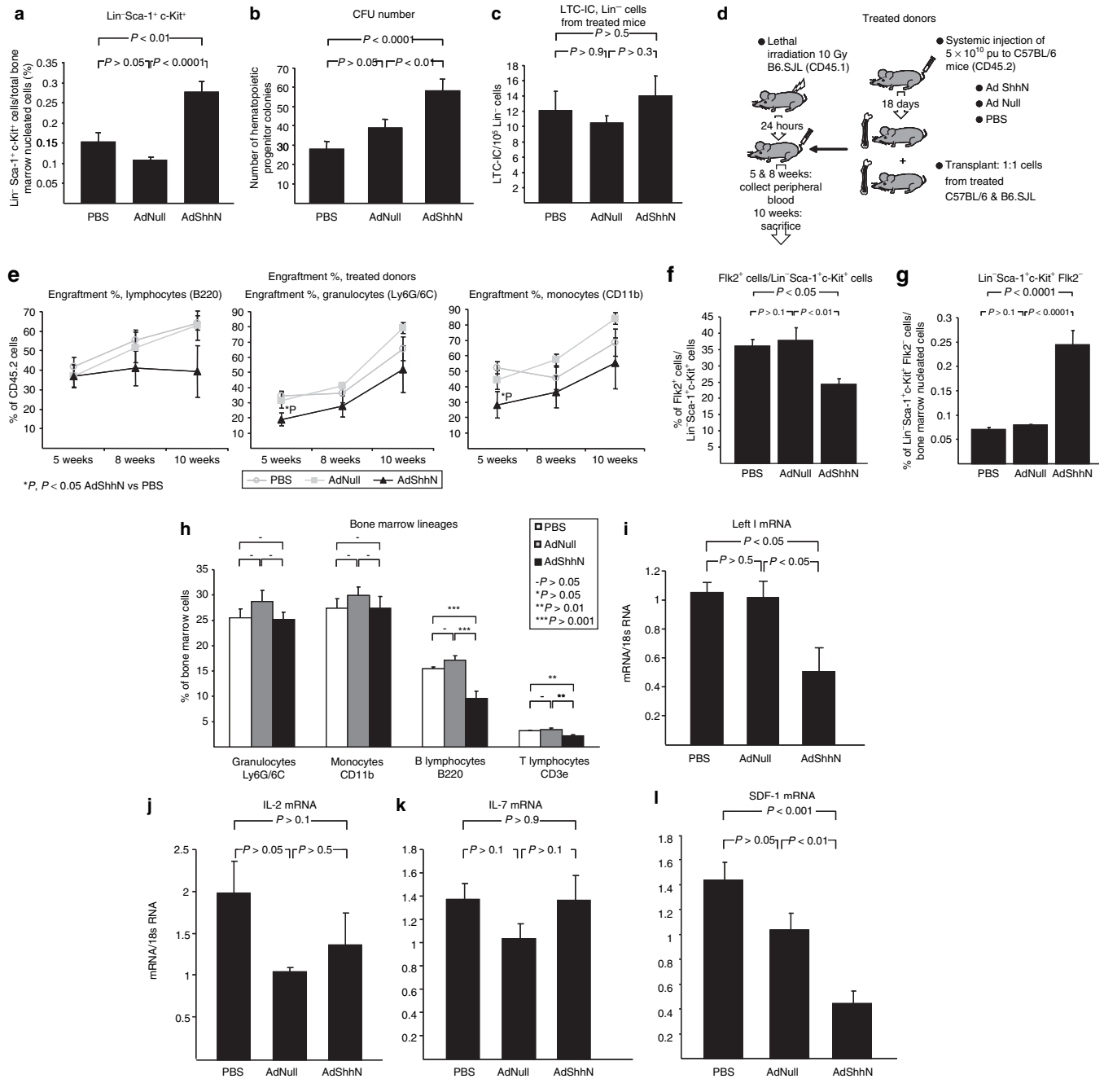

© The American Society of Gene & Cell Therapy

decreased in Shh-treated mice (Figure 3i; $P < 0.05$, AdShhN versus both controls). To further investigate the mechanism of lymphocytopenia, we determined the bone marrow expression levels of stromal-derived growth factor 1 (SDF-1), interleukin 2 (IL-2), and IL-7, all of which are essential factors in lymphopoiesis, SDF-1 being the earliest acting on the pre-pro-B cells.[34] Although the expression levels of IL-2 and IL-7 did not change in the Shh-treated mice (Figure 3j,k; $P > 0.1$, AdShhN versus both controls), there was a significant 60% decrease in the expression of SDF-1 (Figure 3l; $P < 0.001$, AdShhN versus PBS; $P < 0.01$, AdShhN versus AdNull). As SDF-1 is also an important factor for stem cell homing in the bone marrow,[36] we investigated whether the decrease in marrow SDF-1 expression in AdShhN-treated mice was associated with an increase in hematopoietic stem/progenitor cell mobilization. Consistent with this concept, the percentage of Lin^- c-Kit^+ cells, which contain the population of hematopoietic stem/progenitors cells, was significantly increased in peripheral blood (**Supplementary Figure S6a**; $P < 0.05$, AdShhN versus PBS; $P < 0.01$, AdShhN versus AdNull). As the percentage Lin^- Sca-1^+ c-Kit^+ cells did not change (**Supplementary Figure S6b**; $P > 0.5$, AdShhN versus both controls), the increase was due to Lin^- Sca-1^- c-Kit^+ cells (**Supplementary Figure S6c**; $P < 0.05$, AdShhN versus PBS; $P < 0.01$, AdShhN versus AdNull).

To examine the effects of Shh on other adult HSC niches, we performed a histological analysis of the spleens of Shh-treated mice. The analysis showed a 50% increase in the number of multinucleated megakaryocytes in the spleen (**Supplementary Table S1**; $P < 0.01$, AdShhN compared to both controls), suggestive of extramedullary hematopoiesis. No change was detected in the number or size of the germinal centers, indicating no major effect on mature lymphocytes (see **Supplementary Figure S7** for examples of spleen histology; **Supplementary Table S1**; $P > 0.1$, AdShhN versus both controls) (see **Supplementary Materials and Methods**). The Shh-treated spleens were also characterized by an increase in fibroblastic-appearing cells, suggestive of the possibility that a stimulation of the stromal compartment may be responsible for the extramedullary hematopoiesis.

Together, these findings demonstrate that overexpression of Shh causes an increase in bone marrow Lin^- Sca-1^+ c-Kit^+ cells with characteristics of increased hematopoietic progenitor function and a decrease in bone marrow B- and T-lymphocyte numbers with a decrease in the expression of Lef1 and SDF-1. Together with a decrease in Flk2-expressing Lin^- Sca-1^+ c-Kit^+ cells, the decrease in SDF-1 expression suggests that the Shh-mediated defect in lymphopoiesis likely affects the earliest stage of lymphocyte development.

AdShhN treatment induces a functional change in the bone marrow hematopoietic niche *in vivo* resulting in lymphocyte depletion

As we detected extensive changes in the structure of the bone marrow niche accompanied by an increase in hematopoietic progenitors and a decrease in bone marrow lymphocytes, we sought to elucidate whether this was due to a microenvironment-induced mechanism. To investigate this, we first transplanted cells from PBS-, AdNull-, or AdShhN-treated C57BL/6 mice into wild-type B6.SJL recipients (see Figure 3d for experimental design). Consistent with a microenvironment-induced effect, there were no differences in engraftment (Figure 3e; $P > 0.05$ AdShhN versus both controls) or peripheral blood cell counts (Figure 4a; $P > 0.05$ AdShhN versus both controls). Next, we transplanted bone marrow cells from naive B6.SJL donor mice to lethally irradiated C57BL/6 recipients treated with PBS, AdNull, or AdShhN (see Figure 4b for experimental design). Corresponding to an increase in LTC-IC frequency when naive Lin^- cells were cultured on stromal cells from Shh-treated mice (**Supplementary Figure S8**; $P < 0.01$ AdShhN versus PBS; $P < 0.001$, AdShhN versus AdNull), we detected small but statistically significant differences in donor cell engraftment. Engraftment increased in granulocyte population in AdShhN-treated recipients 5 and 8 weeks after transplantation (Figure 4c; $P < 0.01$ AdShhN compared to both controls) and in monocyte population 8 weeks after transplantation (Figure 4c; $P < 0.01$ AdShhN versus both controls). By contrast, engraftment decreased in lymphocyte population in AdShhN-treated recipients 5, 8, and 10 weeks after transplantation (Figure 4c; $P < 0.01$ AdShhN versus both controls). Furthermore, there was a striking 80% decrease in lymphocyte number in peripheral blood (Figure 4d; $P < 0.0001$ AdShhN compared to both controls) leading to a dramatic decrease in total peripheral blood cell counts (Figure 4d; $P < 0.001$ AdShhN versus both controls) while other lineages were comparable with control animals (Figure 4d; $P > 0.05$ AdShhN versus both controls). Similar decrease in

Figure 3 Increase in primitive bone marrow hematopoietic compartment and decrease in bone marrow B and T lymphocytes by elevated levels of Sonic hedgehog (Shh). (**a**) Percentage of Lin^- Sca-1^+ c-Kit^+ (LSK) cells/total bone marrow nucleated cells ($n = 9$, each condition). Femoral bone marrow cells were harvested 18 days after AdShhN vector administration and stained with antibodies against lineage markers (CD3e for T cells, CD11b for monocytes, CD45R for B cells, TER119 for erythrocytes, Ly6G/6C for granulocytes; combination of all markers defined as "Lin") and antibodies against stem cell markers Sca-1 and c-Kit and analyzed by flow cytometry. (**b**) Number of hematopoietic progenitor colonies assessed by colony-forming unit assay ($n = 5$ each condition, each sample in triplicate). Femoral bone marrow cells were harvested 18 days after AdShhN vector administration and plated in methylcellulose medium for colony-forming unit assay. (**c**) Long-term culture-initiating cell (LTC-IC) assay. Lin^- bone marrow cells were isolated from bone marrow of phosphate-buffered saline (PBS) ($n = 4$), AdNull ($n = 4$), or AdShhN-treated ($n = 4$) mice 18 days after vector administration and plated on irradiated naive bone marrow stromal cells in limiting dilutions in LTC-IC assays. (**d,e**) Competitive repopulation assay. B6.SJL (CD45.1) mice were lethally irradiated and transplanted with a 1:1 mixture of bone marrow cells from C57BL/6 (CD45.2) mice treated 18 days before with PBS, AdNull, or AdShhN and wild-type B6.SJL mice (PBS cells, $n = 4$; AdNull cells, $n = 4$; AdShhN cells, $n = 5$). (**d**) Schematic representation of the experimental design; and (**e**) percentage of donor cells in different lineages in peripheral blood 5 and 8 weeks after transplantation and in bone marrow 10 weeks after transplantation. (**f,g**) Flk2 expression in the LSK population. (**f**) $Flk2^+$ cells/LSK cells; and (**g**) percentage of $Flk2^-$ LSK cells/total bone marrow nucleated cells. (**h**) Percentage of hematopoietic lineages in the bone marrow. Bone marrow cells were stained with antibodies against lineage markers (Ly6G/6C for granulocytes, CD11b for monocytes, CD45R for B cells, and CD3e for T cells) and analyzed by flow cytometry ($n = 9$, each condition). (**i–l**) Bone marrow mRNA expression of regulators of lymphoid development. (**i**) Lef1, (**j**) IL-2, (**k**) IL-7, and (**l**) SDF-1. RNA was extracted from bone marrow cells and relative quantification of gene expression was analyzed by TaqMan real-time PCR (PBS, $n = 5$; AdNull, $n = 4$; AdShhN, $n = 5$). For **a–c** and **e–l**, data shown as mean ± SE. Ad, adenovirus; IL-2, interleukin 2; Lef1, lymphoid enhancer–binding factor 1; SDF-1, stromal-derived growth factor 1.

© The American Society of Gene & Cell Therapy

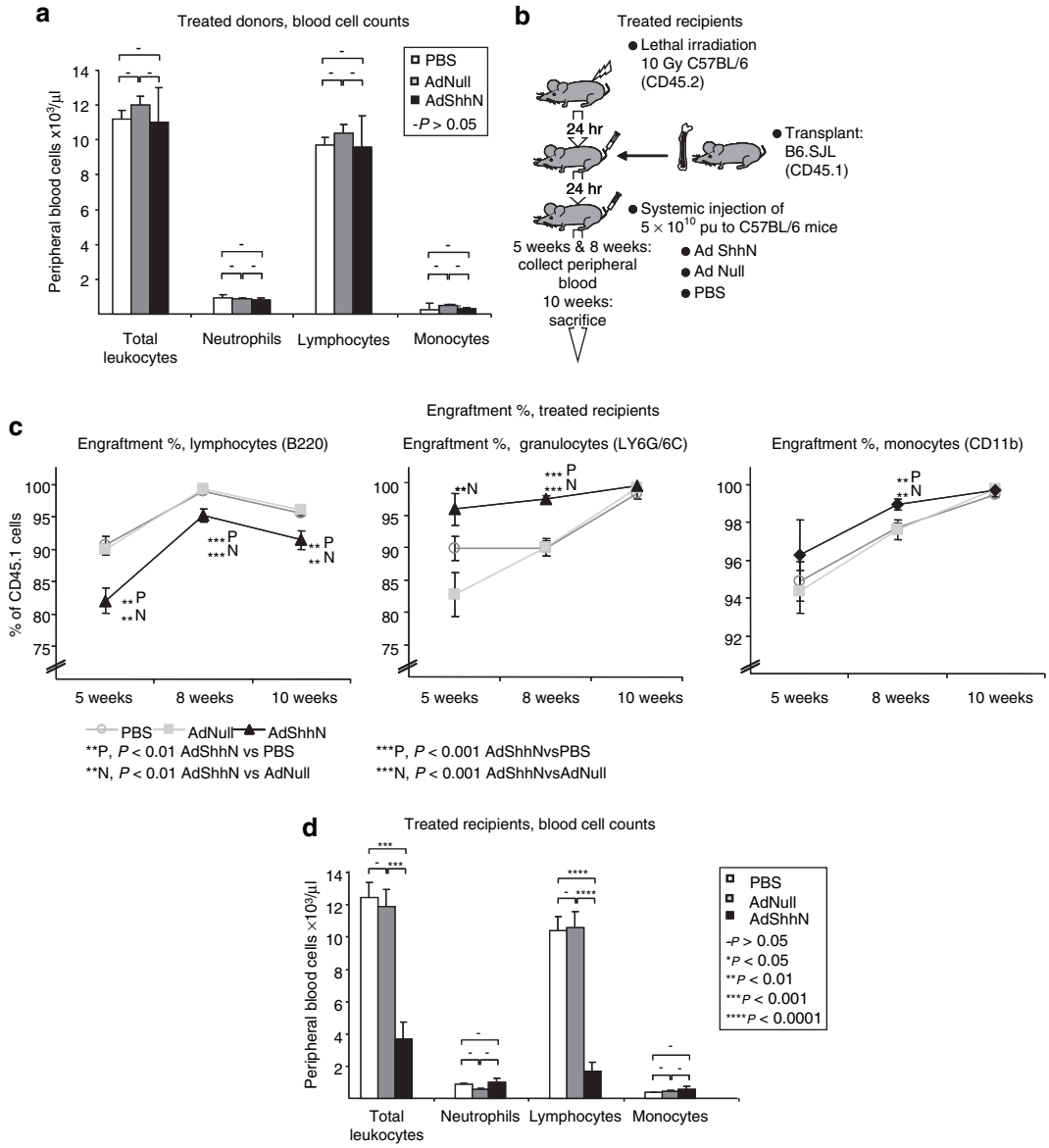

Figure 4 Microenvironment-induced depletion of lymphocytes after bone marrow transplantation and AdShhN treatment. Naive (untreated) B6.SJL mice were lethally irradiated and transplanted with bone marrow cells from C57BL/6 mice treated 18 days before with either phosphate-buffered saline (PBS), AdNull, or AdShhN (PBS cells, $n = 4$; AdNull cells, $n = 4$; AdShhN cells, $n = 5$) (**a**) or C57BL/6 mice were lethally irradiated and transplanted with cells from naive B6.SJL mice and treated with either PBS ($n = 6$), AdNull ($n = 6$), or AdShhN ($n = 5$) (**b–d**). (**a**) Peripheral blood cell counts 8 weeks after transplantation in mice transplanted with cells from PBS-, AdNull-, or AdShhN-treated donors (see **Figure 3c** for experimental design); (**b**) schematic representation of the experimental design of bone marrow transplantation and treatment of recipients with PBS, AdNull, or AdShhN; (**c**) percentage of donor cells in different lineages in peripheral blood 5 and 8 weeks after transplantation and in bone marrow 10 weeks after transplantation in recipients treated with PBS, AdNull, or AdShhN; and (**d**) peripheral blood cell counts 8 weeks after transplantation in recipients treated with PBS, AdNull, or AdShhN. Data shown as mean ± SE. Ad, adenovirus; Shh, Sonic hedgehog.

lymphocytes was detected in the bone marrow of Shh-treated recipients (**Supplementary Figure S9**; $P < 0.01$ AdShhN versus both controls). Together, these data suggest that Shh mediates a functional change in the bone marrow microenvironment *in vivo* that results in a striking decrease in lymphocyte number likely due to impaired lymphoid differentiation of HSCs.

DISCUSSION

This study demonstrates that transient overexpression of Shh mediates structural and functional changes in the bone marrow hematopoietic microenvironment, which leads to depletion of lymphocytes in the bone marrow. The structural alterations are suggestive of an expanded HSC niche, including the appearance of new trabeculae in the diaphyseal bone, with accompanying increases in the osteoblast number and tissue mineralization. Although the overall mineralization decreased in the metaphysis, an area of pre-existing trabeculae, this was also due to an increase in the trabecular surface area, site of the hematopoietic niche. Secondary to these structural changes in the niche, the Shh-treated mice displayed an elevation in the bone marrow Lin^- $Sca\text{-}1^+$ $c\text{-}Kit^+$ cell number with increased hematopoietic progenitor function, surprisingly, however, the functional *in vivo* repopulating stem

© The American Society of Gene & Cell Therapy

cells were not increased in the wild-type environment. Instead, Shh treatment resulted in a decrease in bone marrow lymphocytes that was accompanied by a decrease in SDF-1, an early regulator of lymphopoiesis, as well as a decrease in Flk2-expressing Lin^- $Sca\text{-}1^+$ $c\text{-}Kit^+$ cells, which contain the common lymphoid progenitors. Finally, Shh treatment of bone marrow recipients, but not donors, resulted in depletion of peripheral blood and bone marrow lymphocytes and decreased lymphoid engraftment, suggesting a microenvironment-induced mechanism likely affecting the early lymphopoiesis.

After systemic administration of Ad via a peripheral vein, the major site of adenoviral transduction is the liver. Protein products expressed by the hepatocytes are secreted into the serum at high levels, mimicking sustained serum release of soluble proteins. As the marrow space is highly vascularized, it is likely that the marrow cells are exposed to the high serum levels, as previously shown in analyzing the effects of Ihh, SDF-1, VEGF, and angiopoietin on bone marrow.[37,38] In this study, we used intravenous administration of an Ad vector coding for the soluble N-terminal form of Shh to achieve systemic overexpression of Shh, which was demonstrated by elevated serum levels of Shh and induction of hair growth. Future studies are needed to make further distinction between the direct and indirect effects of Shh by specific blocking studies.

Although Shh is a known critical regulator of limb development and osteoblastogenesis,[8,9,11–13,15] the present Shh-mediated appearance of bone trabeculae within the diaphysis of the femurs in postnatal animals was a striking finding, as trabeculae are normally present only at the metaphyses of long bones.[39] Mechanically, bone trabeculae distribute mechanical stresses and are usually absent from the diaphyseal bone where the cortical bone serves this function.[39] The unusual location of the Shh-generated trabeculae may suggest that Shh signaling is capable of shifting the function of bone from a mechanical to a hematopoietic function. In support of this concept, trabeculae in the metaphyseal region become smaller, favoring an increase in the surface area (the site of the hematopoietic niche) over tissue mineral density. We have also recently observed similar changes in the trabecular bone of the vertebrae of these mice, where an increase in immature osteoblasts due to ShhN treatment resulted in a secondary increase in bone remodeling.[40] Future examination of the effects of controlled mechanical loading on Shh-treated bone is required to understand better the ramification of these observed changes.

The increase in trabecular bone formation in the diaphyseal bone marrow cavity may have affected the number of bone marrow nucleated cells recovered from Shh-treated mice. To circumvent this problem, alternative methods of bone marrow harvesting include mechanic and enzymatic digestion for the osteopetrotic mouse model and for harvesting endosteal HSCs.[41] However, as Shh-treated bone is not osteopetrotic as demonstrated by our micro-computed tomography results, other explanations for the decreased number of cells include the defect in lymphopoiesis affecting the total marrow cell number or the possibility of replicative exhaustion of HSCs as in the patched-deficient mouse, in which Shh pathway signaling is increased.[17] With regard to endosteal HSCs, although harvesting of endosteal HSCs is optimized by the techniques described by Haylock *et al.*,[41] the flushing technique, used as a standard in many studies, likely resulted in similar efficiencies in cell harvesting in Shh-treated and control groups.

Previous studies have demonstrated the expansion or contraction of the HSC niche through changes in osteoblasts.[1–3,23,24,29–31,42,43] In agreement with these previous studies, we observed an increase in Lin^- $Sca\text{-}1^+$ $c\text{-}Kit^+$ cells with enhanced hematopoietic progenitor function in association with Shh treatment, although we did not observe an increase in the functional repopulating cells in wild-type environment *in vivo*. This may seem surprising, particularly as the Shh-treated microenvironment promoted LTC-IC frequency and myeloid engraftment; however, our findings regarding the lymphoid progenitors, as well as previous findings in mice with hedgehog pathway overactivation offer cogent insights into the relevant mechanisms. With regard to Shh effects on the HSCs, our results are consistent with those reported in a study by Trowbridge *et al.*[17] of mice in which hedgehog signaling is overactivated by deletion of one copy of the patched gene.[17] As in our model, the heterozygous patched mice exhibit an increase in Lin^- $Sca\text{-}1^+$ $c\text{-}Kit^+$ cells and hematopoietic progenitors. However, while an initial increase in engraftment and cell cycling of patched heterozygous cells is observed, engraftment and cell cycling eventually decrease due to exhaustion of HSCs.[17] Although the present results showed a decrease in cycling Lin^- cells being consistent with the previous study, an investigation of the cell cycle profile at multiple time points in a more enriched HSC population might show a similar, transient increase. Although the effects of the microenvironment were not investigated by Trowbridge *et al.*,[17] the properties of HSCs appeared cell autonomous. That we did not observe increased engraftment of Shh-treated donor cells may be due to a similar mechanism, *i.e.*, cell-autonomous properties of HSCs, which become evident in a wild-type microenvironment. However, as the donor cells were harvested from AdShhN-treated animals and may have been secondarily affected by the changes in the microenvironment, future investigations are needed to study purely cell-autonomous effects of Shh by a more direct method, such as transducing HSCs *ex vivo* before transplantation.

Although we observed a coordinated increase in osteoblasts and hematopoietic progenitors, overexpression of Shh also affected mature hematopoietic cell composition by mediating a striking reduction in the lymphocyte number, which appeared to be due to a microenvironment-mediated mechanism. AdShhN-treated mice had a decrease in the Flk2-expressing Lin^- $Sca\text{-}1^+$ $c\text{-}Kit^+$ cells, suggesting a deficit in the common lymphoid progenitors.[33,34] In addition, we found a decrease in the expression of Lef1, a transcription factor necessary for lymphoid development,[35] suggesting that this may have occurred due to a block in lymphopoiesis. Consistent with this, we detected a significant decrease in the expression of SDF-1, a factor normally expressed by marrow stromal cells and osteoblasts that support B lymphopoiesis.[44,45] These findings are in agreement with a recent study demonstrating that an inducible ablation of the hedgehog receptor patched and secondary overactivation of hedgehog signaling results in a blockade in the development of T- and B-lymphoid lineages at the level of the common lymphoid progenitor in the bone marrow with a critical involvement of the

© The American Society of Gene & Cell Therapy

stromal cell compartment.[46] Hedgehog proteins have been shown to play a positive regulatory role in the differentiation of thymic T lymphocytes and peripheral B lymphocytes.[47,48] Although the focus of this study was the endosteal bone marrow niche, we also examined the effects of Shh overexpression in the spleen. Histological analysis suggested an increase in extramedullary hematopoiesis in AdShhN-treated mice, but no major effect on mature lymphocytes. The AdShhN-treated spleens were also characterized by an increase in fibroblastic-appearing cells, suggestive of a stimulation of the stromal compartment. These findings suggest that Shh overexpression may change the interaction between the niche and hematopoietic cells also in the spleen, but further investigation is needed to fully understand the extramarrow effects of Shh. That we have found a suppressive role in the bone marrow may reflect the different roles of Shh in lymphopoiesis in the peripheral lymphoid organs compared to the bone marrow. Our findings suggest that in the bone marrow, microenvironment-mediated effects of Shh predominate, leading to decreases in lymphoid progenitor engraftment and differentiation.

Multiple types of niches likely coexist to provide different stem cell–niche functions, such as self-renewal,[3] as well as differentiation.[44,45] Furthermore, the network of multiple stromal cell types, including osteoblasts, endothelial cells, and other stromal cells, is likely critical in establishing the niches.[36,45] The impact of developmental stages of osteoblasts may play a role in the niche function.[25] This study demonstrates that Shh alters the interaction between the microenvironment and the hematopoietic cells altering the maintenance of hematopoietic progenitors and differentiation of their lymphoid progeny, providing a basis to further explore the mechanisms through which these interactions occur. Furthermore, as drugs depleting lymphocytes are used for treatment of B-cell malignancies and autoimmune diseases, it remains to be explored whether mediators of the Shh microenvironment–induced lymphocytopenia could be exploited in the development of future therapies.

MATERIALS AND METHODS

Gene transfer vectors. All Ad vectors were serotype 5 and replication deficient, with deletions in the E1a, E1b, and E3 regions of the Ad genome.[49] The expression cassette of AdShhN contains the cytomegalovirus promoter/enhancer and codes for N-terminal portion of murine Shh, with a stop codon introduced to terminate translation downstream of the glycine residue at position 198 of the Shh peptide.[20] The Ad vector used as a control was AdNull, a vector identical to AdShhN but lacking a cDNA coding sequence. The vectors were propagated in human embryonic kidney 293 cells, purified through 2 CsCl gradients, and characterized with respect to particle concentration (particle units, pu) and transgene expression.[49]

Experimental animals. C57BL/6 male mice 6–8-week old (Jackson Laboratories, Bar Harbor, ME or Taconic, Germantown, NY) were administered into the lateral tail vein with PBS, AdNull 5×10^{10} pu, or AdShhN 5×10^{10} pu in 100 µl volume diluted in PBS. Unless otherwise stated, all mice were killed by CO_2 asphyxiation 18 days after vector administration under an approved institutional animal committee protocol.

Bone histology. Femurs were fixed with 4% paraformaldehyde for 48 hours, decalcified, embedded in paraffin, sectioned, and stained with hematoxylin and eosin (Histoserv, Germantown, MD). To measure area and perimeter of the trabecular bone and tortuosity ratio of the endosteal surface (endosteal surface length divided by bone length), five fields/femoral diaphysis and six fields/endosteal surface of hematoxylin and eosin–stained slides were imaged by brightfield microscopy and images analyzed using MetaMorph imaging software (Universal Imaging, Downingtown, PA).

Immunofluorescence and immunohistochemistry. Incubation with a mouse anti-procollagen type I (SP1.D8; 1:100 dilution; Developmental Studies Hybridoma Bank, University of Iowa, Iowa City, IA), a rabbit anti-human N-cadherin antibody (clone YS; 1:250 dilution; Immuno-Biological Laboratories, Minneapolis, MN), and a goat polyclonal anti-osteopontin antibody (Santa Cruz, Palo Alto, CA) was carried out at +4 °C overnight. Procollagen staining was visualized by incubation with a goat anti-mouse Cy5 conjugated AffiniPure F(ab′)2 (1:100 dilution; Jackson ImmunoResearch, West Grove, PA), N-cadherin staining was visualized with the Vectastain Elite Rabbit ABC kit and osteopontin with the Vectastain Elite Goat ABC kit (Vector Laboratories, Burlingame, CA).

Micro-computed tomography of bone. Femurs were harvested 18 days after vector administration and imaged in a micro-computed tomography scanner (MS-8 Small Specimen Scanner; GE Medical Systems, London, Ontario, Canada) along with a standard SB3 (a polymer with an X-ray attenuation equivalent to bovine cortical bone, 1.1 g of hydroxyapatite/ml) phantom (GE Medical Systems). 3D images were reconstructed at 17 µm isotropic resolution (EVS Beam and eXplore Reconstruction Utility softwares; GE Medical Systems). The inclusion of a standard was used for conversion of the attenuation values to bone mineral density (mg/ml; GEHC Microview Software; GE Medical Systems). Threshold was set to 2,500 for cortical analysis and 800 for trabecular analysis and using the threshold data, inner perimeter and tissue mineral density (excluding cortical bone) in the femoral diaphysis were separately analyzed (GEHC Microview software; GE Medical Systems).

Quantitative PCR. Total tibial bone marrow was flushed out 18 days after vector administration and RNA extracted using TRIzol (Invitrogen, Grand Island, NY) and RNeasy MinElute Cleanup Kit (Invitrogen), and first strand cDNA synthesized using Superscript First Strand Synthesis System for reverse transcriptase–PCR (Invitrogen). Gene expression assays for TaqMan real-time reverse transcriptase–PCR analysis included primers and probes for Runx2, osteopontin, angiopoietin-1, Jagged 1, Lef1, IL-2, IL-7, and SDF-1 (Applied Biosystems, Foster City, CA).

Flow cytometry. Femoral and tibial marrow cells were flushed out with equal amounts/bone of minimal essential medium α (Invitrogen) with 2% fetal bovine serum (Invitrogen) and filtered through a 100-µm cell separator (BD Biosciences, San Jose, CA) as described by Spangrude *et al.*[50] Marrow nucleated cells were blocked with 5% rat serum on ice and stained with a lineage (Lin) antibody cocktail conjugated with allophycocyanin including anti-CD3e (T lymphocytes), anti-CD45R (B lymphocytes), anti-CD11b (monocytes), anti-TER119 (erythrocytes), and anti-Ly6G/6C (granulocytes) antibodies (BD Biosciences Pharmingen, San Jose, CA) followed by staining with anti-Sca-1-FITC, anti-c-Kit-PE (BD Biosciences Pharmingen), Flk2-PE-Cy5, and CD34-PE-Cy7 antibodies with corresponding isotype controls. For analysis of marrow lineages, cells were stained with allophycocyanin-conjugated antibodies against CD3e, CD45R, CD11b, and Ly6G/6C. For cell cycle analysis, cells were stained with Lin antibody cocktail, fixed and permeabilized in 4% paraformaldehyde and 70% ice-cold ethanol, and stained with propidium iodide. To quantify engraftment of donor cells in bone marrow transplant recipients, peripheral blood or bone marrow mononuclear cells were blocked with 5% rat serum on ice and stained with anti-CD45.1-PE and anti-CD45.2-FITC antibodies (BD Biosciences Pharmingen, San Jose, CA) followed by staining with allophycocyanin-conjugated anti-lineage markers (CD45R, CD11b, Ly6G/6C). Cells were acquired on a FACScalibur cytometer (BD Biosciences Pharmingen) using Cell Quest software and analyzed using FlowJo software (BD Biosciences Pharmingen).

© The American Society of Gene & Cell Therapy

Colony-forming unit assay for hematopoietic progenitors. To quantify the number of bone marrow hematopoietic progenitors, femoral bone marrow was harvested from PBS-, AdNull-, and AdShhN-treated animals 18 days after vector administration, and 2×10^4 nucleated cells were plated on 35-mm dishes in triplicate in MethoCult methylcellulose medium containing appropriate cytokines (M3434; StemCell Technologies, Vancouver, British Columbia, Canada). Colonies were scored by brightfield microscopy after 12 days incubation at 37 °C and 5% CO_2.

LTC-IC assay. The modified LTC-IC assay was performed as follows. To establish feeder layers, marrow was harvested from naive and PBS-, AdNull-, and AdShhN-treated mice 18 days after vector administration and cell suspensions were plated into MyeloCult medium (StemCell Technologies), cultured at 33 °C and 5% CO_2, and irradiated at 80% confluency. To prepare Lin^- cells, marrow of either PBS-, AdNull-, and AdShhN-treated animals or naive mice were harvested, Lin^- cells were enriched by magnetic beads (Miltenyi Biotec, Auburn, CA) and then plated on feeder layers (naive Lin^- cells on feeder layers from PBS-, AdNull-, and AdShhN-treated mice or Lin^- cells from PBS-, AdNull-, and AdShhN-treated mice on naive feeder layers) in limiting dilutions from 6,000 to 1,500 cells/well in eight wells each and cultured for 5 weeks at 33 °C and 5% CO_2 with weekly half-medium changes. Thereafter medium was replaced with 100 µl MethoCult medium and colonies were scored after 10-day incubation at 33 °C and 5% CO_2. LTC-IC frequencies were calculated using L-Calc software (Stem Cell Technologies).

Bone marrow transplantation. Transplantation assays were performed to assess bone marrow repopulation ability and microenvironment-induced effects. First, recipient B6.SJL mice (strain B6.SJLPtprc<a>; CD45.1; 7–10-week-old; male; Jackson Laboratories) were irradiated with 10 Gy 24 hours before transplantation. The bone marrow donor cells were obtained from C57BL/6 mice (CD45.2; 7–10-week-old; male) treated 18 days before with PBS, AdNull, or AdShhN (prepared as described in the Flow Cytometry section). In each group, the cells were pooled from three donors. A mixture of equal amounts of the PBS-, AdNull-, or AdShhN-treated C57BL/6 bone marrow cells along with B6.SJL bone marrow cells were injected intravenously into the recipients. Second, recipient C57BL/6 mice (CD45.2; 7–10-week-old; male) were irradiated with 10 Gy 24 hours before transplantation. The bone marrow donor cells were obtained from B6.SJL mice (CD45.1; 7–10-week-old; male) and were injected intravenously into the recipients. After 24 hours, the recipients were injected intravenously with PBS, AdNull 5×10^{10} pu, or AdShhN 5×10^{10} pu. In both experiments described, the mice were bled 5 and 8 weeks after transplantation and killed 10 weeks after transplantation for analysis of engraftment and differential blood cell counts.

Peripheral blood analysis. Retro-orbital blood was collected 5 and 8 weeks after bone marrow transplantation with microcapillary tubes (Fischer Scientific, Pittsburgh, PA). Differential blood counts were obtained using an automated Bayer Advia 120 MultiSpecies Hematology Analyzer (Bayer HealthCare, Tarrytown, NY).

Statistical analysis. All data sets included four to nine animals per group. Groups were compared using analysis of variance. For multiple measurements in the *in vitro* assays and image analyses, data were analyzed with repeated measurement analysis of variance with post hoc testing where differences were detected using StatView software (SAS, Cary, NC). Significance was accepted where $P < 0.05$. Results are expressed as mean ± SEM.

SUPPLEMENTARY MATERIAL

Table S1. Spleen analyses.
Figure S1. Demonstration of the function of the AdShhN vector.
Figure S2. Reversal of bone phenotype in AdShhN-treated mice by 8 months after vector administration.
Figure S3. Increased serum levels of osteocalcin in AdShhN-treated mice.
Figure S4. Total number of nucleated cells and Lin^- Sca-1^+ c-Kit^+ cells in the bone marrow after AdShhN treatment.
Figure S5. Characterization of primitive hematopoietic compartment after AdShhN treatment.
Figure S6. Increase in Lin^- c-Kit^+ cells hematopoietic cells in peripheral blood after AdShhN treatment.
Figure S7. Spleen histology demonstrating no change in the number or size of germinal centers in the spleens of AdShhN-treated mice.
Figure S8. Increased capacity of bone marrow stromal cells from AdShhN-treated mice to support long-term culture-initiating cells.
Figure S9. Depletion of lymphocytes in the bone marrow after bone marrow transplantation and AdShhN treatment.
Materials and Methods.

ACKNOWLEDGMENTS

We thank H. Lou, L. Pierre-Destine, C. Cheng, A. Bajak, E. Gancher, S. Damle, E. DiCarlo, L. Lukashova, S.B. Doty, and N.R. Hackett for their assistance in the study; M.A.S. Moore for helpful discussions; and T. Virgin-Bryan and N. Mohamed for assistance with preparation of the manuscript. This work was supported, in part, by the National Institutes of Health grant P01 HL59312 and the Will Rogers Memorial Fund, Los Angeles, CA and M.K., in part, by the Sigrid Juselius Fellowship, the Finnish Medical Foundation, and the Maud Kuistila Memorial Foundation.

REFERENCES

1. Adams, GB and Scadden, DT (2006). The hematopoietic stem cell in its place. *Nat Immunol* **7**: 333–337.
2. Moore, KA and Lemischka, IR (2006). Stem cells and their niches. *Science* **311**: 1880–1885.
3. Wilson, A and Trumpp, A (2006). Bone-marrow haematopoietic-stem-cell niches. *Nat Rev Immunol* **6**: 93–106.
4. Gong, JK (1978). Endosteal marrow: a rich source of hematopoietic stem cells. *Science* **199**: 1443–1445.
5. Bhardwaj, G, Murdoch, B, Wu, D, Baker, DP, Williams, KP, Chadwick, K *et al.* (2001). Sonic hedgehog induces the proliferation of primitive human hematopoietic cells via BMP regulation. *Nat Immunol* **2**: 172–180.
6. Nilsson, SK, Haylock, DN, Johnston, HM, Occhiodoro, T, Brown, TJ and Simmons, PJ (2003). Hyaluronan is synthesized by primitive hemopoietic cells, participates in their lodgment at the endosteum following transplantation, and is involved in the regulation of their proliferation and differentiation *in vitro*. *Blood* **101**: 856–862.
7. Adams, GB, Martin, RP, Alley, IR, Chabner, KT, Cohen, KS, Calvi, LM *et al.* (2007). Therapeutic targeting of a stem cell niche. *Nat Biotechnol* **25**: 238–243.
8. Chiang, C, Litingtung, Y, Lee, E, Young, KE, Corden, JL, Westphal, H *et al.* (1996). Cyclopia and defective axial patterning in mice lacking Sonic hedgehog gene function. *Nature* **383**: 407–413.
9. Kinto, N, Iwamoto, M, Enomoto-Iwamoto, M, Noji, S, Ohuchi, H, Yoshioka, H *et al.* (1997). Fibroblasts expressing Sonic hedgehog induce osteoblast differentiation and ectopic bone formation. *FEBS Lett* **404**: 319–323.
10. Dyer, MA, Farrington, SM, Mohn, D, Munday, JR and Baron, MH (2001). Indian hedgehog activates hematopoiesis and vasculogenesis and can respecify prospective neurectodermal cell fate in the mouse embryo. *Development* **128**: 1717–1730.
11. Jemtland, R, Divieti, P, Lee, K and Segre, GV (2003). Hedgehog promotes primary osteoblast differentiation and increases PTHrP mRNA expression and iPTHrP secretion. *Bone* **32**: 611–620.
12. McMahon, AP, Ingham, PW and Tabin, CJ (2003). Developmental roles and clinical significance of hedgehog signaling. *Curr Top Dev Biol* **53**: 1–114.
13. Alzghoul, MB, Gerrard, D, Watkins, BA and Hannon, K (2004). Ectopic expression of IGF-I and Shh by skeletal muscle inhibits disuse-mediated skeletal muscle atrophy and bone osteopenia *in vivo*. *FASEB J* **18**: 221–223.
14. Gering, M and Patient, R (2005). Hedgehog signaling is required for adult blood stem cell formation in zebrafish embryos. *Dev Cell* **8**: 389–400.
15. Edwards, PC, Ruggiero, S, Fantasia, J, Burakoff, R, Moorji, SM, Paric, E *et al.* (2005). Sonic hedgehog gene-enhanced tissue engineering for bone regeneration. *Gene Ther* **12**: 75–86.
16. Trowbridge, JJ, Xenocostas, A, Moon, RT and Bhatia, M (2006). Glycogen synthase kinase-3 is an *in vivo* regulator of hematopoietic stem cell repopulation. *Nat Med* **12**: 89–98.
17. Trowbridge, JJ, Scott, MP and Bhatia, M (2006). Hedgehog modulates cell cycle regulators in stem cells to control hematopoietic regeneration. *Proc Natl Acad Sci USA* **103**: 14134–14139.
18. Kobune, M, Ito, Y, Kawano, Y, Sasaki, K, Uchida, H, Nakamura, K *et al.* (2004). Indian hedgehog gene transfer augments hematopoietic support of human stromal cells including NOD/SCID-beta2m-/- repopulating cells. *Blood* **104**: 1002–1009.
19. Mandal, L, Martinez-Agosto, JA, Evans, CJ, Hartenstein, V and Banerjee, U (2007). A Hedgehog- and Antennapedia-dependent niche maintains Drosophila haematopoietic precursors. *Nature* **446**: 320–324.

© The American Society of Gene & Cell Therapy

20. Lou, H, Crystal, RG and Leopold, PL (2005). Enhanced efficacy of cholesterol-minus sonic hedgehog in postnatal skin. *Mol Ther* **12**: 575–578.
21. Sato, N, Leopold, PL and Crystal, RG (1999). Induction of the hair growth phase in postnatal mice by localized transient expression of Sonic hedgehog. *J Clin Invest* **104**: 855–864.
22. Roelink, H, Porter, JA, Chiang, C, Tanabe, Y, Chang, DT, Beachy, PA *et al*. (1995). Floor plate and motor neuron induction by different concentrations of the amino-terminal cleavage product of sonic hedgehog autoproteolysis. *Cell* **81**: 445–455.
23. Calvi, LM, Adams, GB, Weibrecht, KW, Weber, JM, Olson, DP, Knight, MC *et al.* (2003). Osteoblastic cells regulate the haematopoietic stem cell niche. *Nature* **425**: 841–846.
24. Zhang, J, Niu, C, Ye, L, Huang, H, He, X, Tong, WG *et al.* (2003). Identification of the haematopoietic stem cell niche and control of the niche size. *Nature* **425**: 836–841.
25. Aguila, HL and Rowe, DW (2005). Skeletal development, bone remodeling, and hematopoiesis. *Immunol Rev* **208**: 7–18.
26. Ducy, P, Schinke, T and Karsenty, G (2000). The osteoblast: a sophisticated fibroblast under central surveillance. *Science* **289**: 1501–1504.
27. Kiel, MJ, Radice, GL and Morrison, SJ (2007). Lack of evidence that hematopoietic stem cells depend on N-cadherin-mediated adhesion to osteoblasts for their maintenance. *Cell Stem Cell* **1**: 204–217.
28. Adams, GB, Chabner, KT, Alley, IR, Olson, DP, Szczepiorkowski, ZM, Poznansky, MC *et al.* (2006). Stem cell engraftment at the endosteal niche is specified by the calcium-sensing receptor. *Nature* **439**: 599–603.
29. Nilsson, SK, Johnston, HM, Whitty, GA, Williams, B, Webb, RJ, Denhardt, DT *et al.* (2005). Osteopontin, a key component of the hematopoietic stem cell niche and regulator of primitive hematopoietic progenitor cells. *Blood* **106**: 1232–1239.
30. Stier, S, Ko, Y, Forkert, R, Lutz, C, Neuhaus, T, Grünewald, E *et al.* (2005). Osteopontin is a hematopoietic stem cell niche component that negatively regulates stem cell pool size. *J Exp Med* **201**: 1781–1791.
31. Arai, F, Hirao, A, Ohmura, M, Sato, H, Matsuoka, S, Takubo, K *et al.* (2004). Tie2/angiopoietin-1 signaling regulates hematopoietic stem cell quiescence in the bone marrow niche. *Cell* **118**: 149–161.
32. Christensen, JL and Weissman, IL (2001). Flk-2 is a marker in hematopoietic stem cell differentiation: a simple method to isolate long-term stem cells. *Proc Natl Acad Sci USA* **98**: 14541–14546.
33. Mackarehtschian, K, Hardin, JD, Moore, KA, Boast, S, Goff, SP and Lemischka, IR (1995). Targeted disruption of the flk2/flt3 gene leads to deficiencies in primitive hematopoietic progenitors. *Immunity* **3**: 147–161.
34. Nagasawa, T (2006). Microenvironmental niches in the bone marrow required for B-cell development. *Nat Rev Immunol* **6**: 107–116.
35. Reya, T, O'Riordan, M, Okamura, R, Devaney, E, Willert, K, Nusse, R *et al.* (2000). Wnt signaling regulates B lymphocyte proliferation through a LEF-1 dependent mechanism. *Immunity* **13**: 15–24.
36. Sugiyama, T, Kohara, H, Noda, M and Nagasawa, T (2006). Maintenance of the hematopoietic stem cell pool by CXCL12-CXCR4 chemokine signaling in bone marrow stromal cell niches. *Immunity* **25**: 977–988.
37. Kobune, M, Kato, J, Kawano, Y, Sasaki, K, Uchida, H, Takada, K *et al.* (2008). Adenoviral vector-mediated transfer of the Indian hedgehog gene modulates lymphomyelopoiesis *in vivo*. *Stem Cells* **26**: 534–542.
38. Moore, MA, Hattori, K, Heissig, B, Shieh, JH, Dias, S, Crystal, RG *et al.* (2001). Mobilization of endothelial and hematopoietic stem and progenitor cells by adenovector-mediated elevation of serum levels of SDF-1, VEGF, and angiopoietin-1. *Ann NY Acad Sci* **938**: 36–45; discussion 45.
39. Huiskes, R, Ruimerman, R, van Lenthe, GH and Janssen, JD (2000). Effects of mechanical forces on maintenance and adaptation of form in trabecular bone. *Nature* **405**: 704–706.
40. Kiuru, M, Solomon, J, Ghali, B, van der Meulen, M, Crystal, RG and Hidaka, C (2009). Transient overexpression of sonic hedgehog alters the architecture and mechanical properties of trabecular bone. *J Bone Miner Res*; published online 1 April 2009 (doi:10.1359/jbmr.090313).
41. Haylock, DN, Williams, B, Johnston, HM, Liu, MC, Rutherford, KE, Whitty, GA *et al.* (2007). Hemopoietic stem cells with higher hemopoietic potential reside at the bone marrow endosteum. *Stem Cells* **25**: 1062–1069.
42. Deguchi, K, Yagi, H, Inada, M, Yoshizaki, K, Kishimoto, T and Komori, T (1999). Excessive extramedullary hematopoiesis in Cbfa1-deficient mice with a congenital lack of bone marrow. *Biochem Biophys Res Commun* **255**: 352–359.
43. Visnjic, D, Kalajzic, Z, Rowe, DW, Katavic, V, Lorenzo, J and Aguila, HL (2004). Hematopoiesis is severely altered in mice with an induced osteoblast deficiency. *Blood* **103**: 3258–3264.
44. Tokoyoda, K, Egawa, T, Sugiyama, T, Choi, BI and Nagasawa, T (2004). Cellular niches controlling B lymphocyte behavior within bone marrow during development. *Immunity* **20**: 707–718.
45. Zhu, J, Garrett, R, Jung, Y, Zhang, Y, Kim, N, Wang, J *et al.* (2007). Osteoblasts support B-lymphocyte commitment and differentiation from hematopoietic stem cells. *Blood* **109**: 3706–3712.
46. Uhmann, A, Dittmann, K, Nitzki, F, Dressel, R, Koleva, M, Frommhold, A *et al.* (2007). The Hedgehog receptor Patched controls lymphoid lineage commitment. *Blood* **110**: 1814–1823.
47. Gutierrez-Frias, C, Sacedon, R, Hernandez-Lopez, C, Cejalvo, T, Crompton, T, Zapata, AG *et al.* (2004). Sonic hedgehog regulates early human thymocyte differentiation by counteracting the IL-7-induced development of CD34+ precursor cells. *J Immunol* **173**: 5046–5053.
48. Sacedon, R, Diez, B, Nunez, V, Hernandez-Lopez, C, Gutierrez-Frias, C, Cejalvo, T *et al.* (2005). Sonic hedgehog is produced by follicular dendritic cells and protects germinal center B cells from apoptosis. *J Immunol* **174**: 1456–1461.
49. Rosenfeld, MA, Siegfried, W, Yoshimura, K, Yoneyama, K, Fukayama, M, Stier, LE *et al.* (1991). Adenovirus-mediated transfer of a recombinant alpha 1-antitrypsin gene to the lung epithelium *in vivo*. *Science* **252**: 431–434.
50. Spangrude, GJ, Heimfeld, S and Weissman, IL (1988). Purification and characterization of mouse hematopoietic stem cells. *Science* **241**: 58–62.